Journal of Applied Polymer Science

Synthesis and Characterization of Salep Sulfate and Its Utilization in Preparation of Heavy Metal Ion Adsorbent

Ali Pourjavadi,[1] Malihe Doulabi,[1] Ali Asghar Alamolhoda,[2] Elham Tavakkoli,[1] Shokoufe Amirshekari[1]

[1]Polymer Research Laboratory, Department of Chemistry, Sharif University of Technology, Tehran, Iran

[2]Institute of Water and Energy, Sharif University of Technology, Tehran, Iran

Correspondence to: A. Pourjavadi (E-mail: purjavad@sharif.edu)

ABSTRACT: A multicomponent polysaccharide obtained from dried tubers of certain natural terrestrial orchids was chemically modified by sulfonation using chlorosulfonic acid–dimethylformamide ($HClSO_3$_DMF) complex as a reagent. For a structural characterization of salep sulfate ^1H nuclear magnetic resonance (NMR), Fourier transform infrared (FTIR) spectra, and Thermogravimetric analysis (TGA) curves were recorded. The sulfate content of modified salep was determined using elemental analysis. This modified biopolymer was used to prepare a new environment-friendly heavy metal ion adsorbent, salep sulfate-*graft*-polyacrylic acid hydrogel (SS-*g*-PAA). Swelling rate and equilibrium water absorbency in various pH and saline solutions were investigated to study the effect of salep sulfate on swelling behavior of the hydrogel. In addition, the effect of sulfate content on heavy metal ion adsorption from aqueous solution was investigated. The results show that SS-*g*-PAA can effectively remove heavy metal ions (Co^{2+}, Zn^{2+}, Cu^{2+}) from aqueous solution and swelling behavior of the hydrogels highly dependent on the amount of sulfate group on corresponding modified polysaccharide. © 2013 Wiley Periodicals, Inc. J. Appl. Polym. Sci. 130: 3001–3008, 2013

KEYWORDS: functionalization of polymers; radical polymerization; swelling; adsorption

Received 28 February 2013; accepted 5 May 2013; Published online 17 June 2013

DOI: 10.1002/app.39515

INTRODUCTION

Heavy metals that mainly includes Pb^{2+}, Al^{3+}, Hg^{2+}, Zn^{2+}, Co^{2+}, Cu^{2+}, Cd^{2+}, Ni^{2+}, and so on are dangerous toxins and environmental pollutants. Small amount of some metals are essential for normal function of body but excessive amounts of them in the body can be toxic. After entering the body, heavy metals don't dispose and accumulate in the tissues of the body. This event causes numerous diseases and complications in the body. Heavy metals widely enter into the environment from artificial and natural resources. The entry of heavy metals into the environment is far beyond the level that can be removed by natural processes. So, the accumulation of heavy metals in the environment is significant.[1,2] There are several methods for heavy metals removal from wastewater such as chemical precipitation,[3] solvent extraction,[4] micellar ultrafiltration,[5] organic and inorganic ion exchange,[6] and adsorption.[7–12] Most of these methods are expensive and contain other pollutant additives. Another disadvantage of these methods can be using chemicals that are not biodegradable and will eventually contaminate environment. So, polysaccharide-based hydrogel adsorbents because of their application particularities, such as biocompatibility, biodegradability, lack of toxicity, and high degree of swelling are viewed as a more attractive adsorbent in recent years.[13–16] Because of three-dimensional (3D) structures, hydrogels have been able to absorb and retain large volumes of water and so have been employed in the favorable feature, especially in the treatment of water and industrial wastewater.[17,18] The absorbency of a hydrogel depends not only on the density of cross-links forming the 3D network, but also the nature and the density of the hydrophilic groups. So, the introduction of hydrophilic groups such as sulfate groups on the polysaccharide can improve the properties of corresponding hydrogel.[19–21]

Salep is a powder which can be obtained from dried tubers of certain natural terrestrial orchids. This important product with manifold properties has been used as additives in food and nonfood applications for many years.[22] In the food industry, salep is used for making ice cream and drink and is also applied as a thickening agent, emulsifier, and stabilizer in a wide variety of products. In the pharmacy industry, salep is a very important biocompound. Salep acts as a preventative of chronic disease, and a weight control agent, and is considered to be a useful advance in treatment of chronic constipation in adult patients.[23–25] From a chemical point of view, salep is known to be a valuable source for glucomannan (16–55%) and also has been reported to contain starch (2.7%), nitrogenous substance (5%), moisture (12%), and ash (2.4%).[26] Salep-based

superabsorbent hydrogels that have unique potentials for use in various fields were firstly synthesized and introduced in our lab.[27–32]

During the past several decades, there have been several methods for sulfonation of polysaccharides.[33–36] Among them, the methods are widely regarded that have the least degradation and complete substitution. One of the reagents found useful for sulfonation of polysaccharides including chitosan and cellulose derivatives is complexes of chlorosulfonic acid with *N,N*-dimethylformamide (DMF).[37,38] DMF was found a type of neutral compound most suitable for this purpose because it is readily available and an excellent solvent for a great number of polymers, polysaccharides, and polysaccharide derivatives.[39] In this article, we report new results on the synthesis of salep sulfate using chlorosulfonic acid–DMF ($HClSO_3$–DMF) complex and its characterization regarding the sulfate content and the chemical structure. The salep sulfate with different sulfate content was grafted with acrylic acid (AA) to obtain hydrogels with both high-saline absorbency and high-water absorbency. The effect of sulfate content on the water absorbency in various media and heavy metal ion adsorption from aqueous solution was examined. The results show that salep sulfate-based hydrogel is an effective adsorbent for the removal of heavy metal ions from aqueous solutions.

EXPERIMENTAL

Materials

The palmate-tuber salep ($M_w = 4.225 \times 10^8$ g/mol; $M_n = 4.500 \times 10^6$ g/mol) was purchased from a supplier in Kordestan, Iran. Chlorosulfonic acid, *N,N*-methylenebisacrylamide (MBA), and ammoniumpersulfate (APS) were obtained from Merck company (Darmstadt, Germany). AA (Merck company) was purified by distillation under reduced pressure to remove the inhibitor hydroquinone before use. Solid $Co(NO_3)_2.6H_2O$, $Zn(NO_3)_2.6H_2O$, and $Cu(NO_3)_2.3H_2O$ were purchased from Merck company. All other reagents used were of analytical grade, and all solutions were prepared with deionized water.

Preparation of Salep Sulfates

Sulfonation of salep was performed according to the method of Gamzazade et al.,[40] with several modifications. The sulfating reagent was prepared by dropwise adding $HClSO_3$ to DMF that had been previously cooled to 0°C–4°C. The reaction mixture was then stirred without cooling until the solution reached room temperature. One gram of salep was added to the 30 mL sulfonating reagent and the reaction mixture was stirred overnight at room temperature. The modified polymer was neutralized with 20% NaOH and precipitated in cold MeOH. The obtained precipitate was dried at 50°C.

Preparation of Salep Sulfate-Graft-Poly Acrylic Acid (SS-g-PAA) Hydrogels

A general procedure for chemically cross-linking graft copolymerization of AA onto salep sulfate backbones was conducted as follows. Salep sulfate (50 mg) was added to 30 mL H_2O at a three-neck reactor equipped with a mechanical stirrer (RZR 2021, Heidolph, Schwabach, Germany), while stirring (200 rpm). The reactor was placed in a thermostated water bath preset at desired temperature (70°C) for 10 min. After dissolving SS and homogenizing the mixture, the monomer, AA (3 mL) and the cross-linker, MBA (30 mg in 5 mL H_2O) were simultaneously added and the reaction mixture stirred for further 15 min. Then, the APS initiator (250 mg in 5 mL H_2O) was added and gelation was observed after around 40 min. The gel product was poured into 100 mL of ethanol for 2 h and then scissored to small pieces. The ethanol was decanted and 100 mL fresh ethanol was added. The particles were allowed to stand for 24 h in ethanol to be completely dewatered. The dewatered gel particles were filtered and dried in an oven at 50°C for 24 h. The product was milled and all samples used for test had a particle size in the range of 40–60 mesh. The salep-*graft*-polyacrylic acid (S-*g*-PAA) hydrogel was also prepared according to the above procedure to investigate the effect of sulfate content on water absorbency of the hydrogel.

Characterization

Fourier transform infrared (FTIR) spectra of samples were taken using an ABB Bomem MB-100 FTIR spectrophotometer. The samples were powdered and mixed with KBr to make pellets. Thermogravimetric analysis (TGA) was acquired at a heating rate of 20°C/min under a nitrogen atmosphere with a TGA Q 50 thermogravimetric analyzer. ^1H nuclear magnetic resonance (NMR) spectra were recorded on a Bruker NMR 500 MHz Instrument in D_2O solvent. Sulfate content percentage was measured in a SC-132 sulfur meter (LECO). An atomic absorption spectrometer (Varian AA-5) was used for the measurements of the metal ion concentrations.

Measurement of Equilibrium Water Absorbency and Swelling Rate

One hundred milligrams of the milled hydrogel particles was immersed in 200 mL distilled water for 3 h at room temperature. Swollen samples were then separated from unabsorbed water by filtering through a 100-mesh nylon screen. The equilibrium water absorbency in distilled water of the hydrogel, Q_e (H_2O), was measured using the following formula:

$$Q_e = \frac{(W_2 - W_1)}{W_1} \quad (1)$$

where W_1 and W_2 are the weights of dry and swollen gel, respectively.

Equilibrium water absorbency of the milled hydrogel in NaCl solutions was calculated according to the same procedure. For studying the rate of absorption of the hydrogel, at consecutive time intervals, the swelling of the hydrogel was measured according to the mentioned method. To investigate the swelling variation with pH, the swelling was measured at favored pH solutions instead of distilled water. The various solutions were adjusted to the desired pH value by addition of diluted HCl or NaOH solution.

Adsorption Experiments

Batch experiments were carried out by agitating 50 mg of milled hydrogel particles in 100 mL of metal ion solutions (Co^{2+}, Zn^{2+}, Cu^{2+}, 1000 mg/L) at 150 rpm for 120 min (room

temperature; pH = 7). At the end of the experiment, the mixture was filtered. Then, the heavy metal ion concentration in the filtrate was measured by atomic absorption spectroscopy. The amount of metal ion adsorbed on the hydrogel at adsorption equilibrium, q_e (mg/g), was calculated according to eq. ((2)):

$$q_e = \frac{[(C_0 - C_e)V]}{W} \quad (2)$$

where C_0 and C_e are the initial and equilibrium metal ion concentrations (mg/L), V is the used volume of the metal ion solution (L), and W is the weight of adsorbent used (g), respectively.[41] Data are representative of at least two experiments (standard deviations <5.0%).

RESULTS AND DISCUSSION

Synthesis and Characterization

The results of salep sulfate under different sulfating reagent are shown in Table I. As shown in Table I, the sulfur content shows an increase with the increasing amount of chlorosulfonic acid but with further increasing of chlorosulfonic acid, slight desulfatation reactions can take place. It also can be seen from Table I, an increase in reaction time causes an increase in the degree of sulfate substitution.

Table I. Salep Sulfate Obtained with Different Sulfating Reagent and Reaction Time

Sample code	Reaction time (h)	Chlorosulfonic acid (mol)	Sulfur (%)
SS1	24	2.5	5.225
SS2	24	3	6.055
SS3	24	3.5	4.600
SS4	48	2.5	6.034

Cross-linking graft copolymerization of AA onto salep sulfate was carried out by using of APS as a free radical initiator and MBA as a hydrophilic cross-linker. At the first step, the thermally dissociating initiator, that is, APS, is decomposed under heating (70°C) to produce sulfate anion radical. Then, the radical abstracts hydrogen from the hydroxyl group of the salep sulfate to form alkoxy radicals on the substrate. These macroradicals initiate AA grafting onto salep sulfate backbone led to a graft copolymer. In addition, in the presence of a cross-

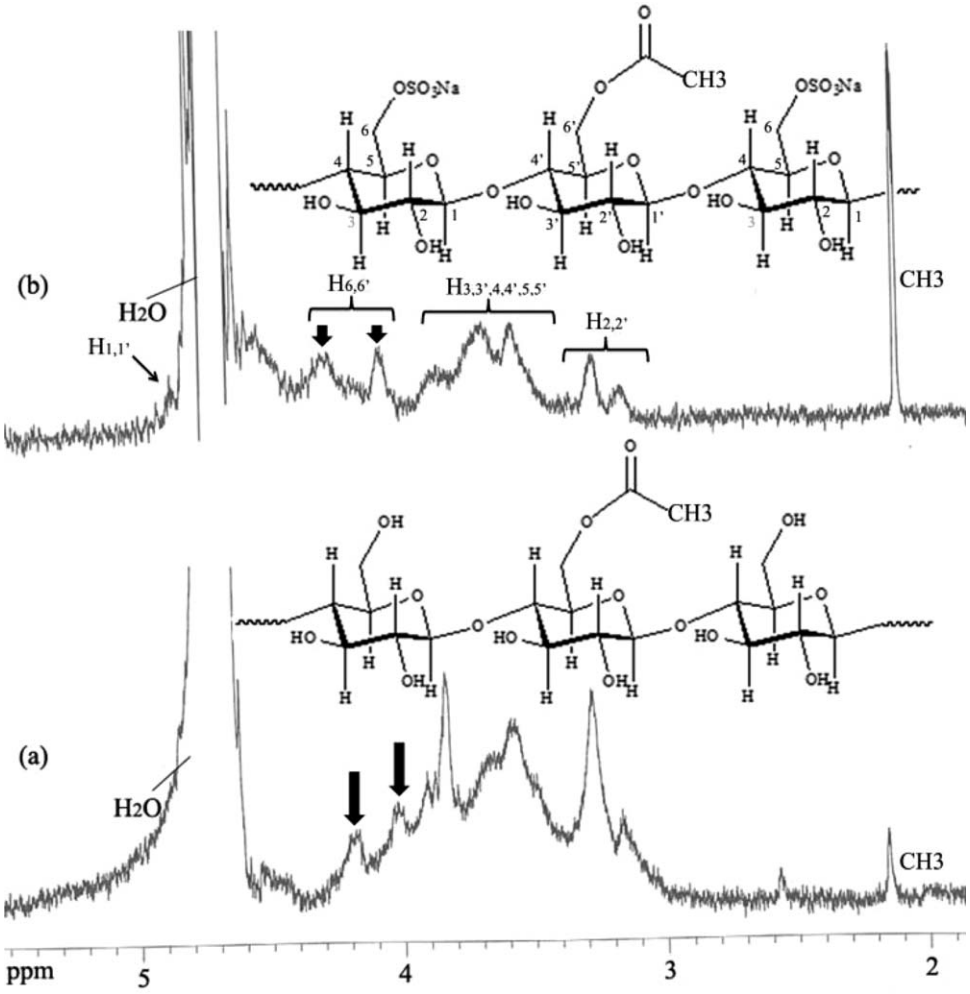

Figure 1. ^{1}H NMR spectra of S (a) and SS2 (b). Solvent = D_2O.

Applied Polymer SCIENCE

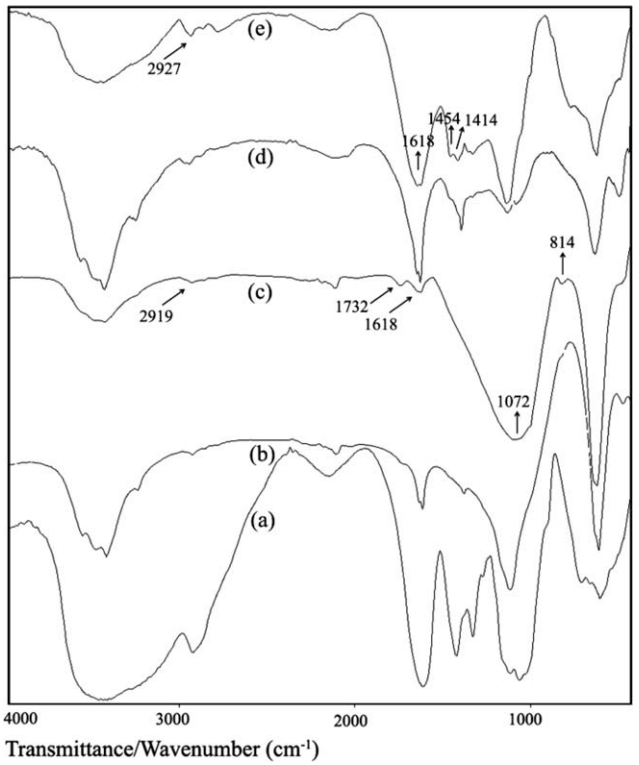

Figure 2. FTIR spectra of S (a), SS1 (b), SS2 (c), S-*g*-PAA (d), and SS2-*g*-PAA (e).

linker, that is, MBA, cross-linking reaction was occurred and finally a cross-linked structure was obtained.[42,43] The swelling degree of cross-linked structure in water is mainly attributed to the characteristics of the external solution, such as charge number, ionic strength, and polymer nature, that is, extent of cross-linking density and presence of hydrophilic functional groups.[44] Thus, the degree of swelling of a salep sulfate-based hydrogel can be expected to be higher than that of the existing salep-based hydrogel.

The structure of salep sulfate was investigated by means of ^{1}H NMR and FTIR spectroscopy (Figures 1 and 2). In the ^{1}H NMR spectrum (Figure 1), the signals of the parent salep at 4.013 and 4.159 ppm are assigned to the CH_2 groups of the C-6 hydroxyl group. After sulfonation, the two peaks of salep are shifted to low field at 4.064 and 4.262 ppm, respectively. This result indicates that the C-6 hydroxyl groups are completely sulfated.

The FTIR spectra of salep (S), salep sulfate (SS1 and SS2), S-*g*-PAA, and salep sulfate (SS2)-*g*-PAA are shown in Figure 2. In the FTIR spectrum of salep sulfates, the following characteristic bands are observed, namely, (i) a broad band at 3200–3400 cm^{-1} corresponding to OH groups; (ii) a band at 2915 cm^{-1} attributed to CH_2 groups; (iii) characteristic band at 1618 cm^{-1} owing the stretching band of the C=O group in the glucomannan backbone; (iv) a large band at 1000–1450 cm^{-1} for C–O–C, CH_2, C–OH, and S=O stretching; and (v) a band at 814 cm^{-1} for S–O stretching from the sulfated glucosidic units. As indicated in Figure 2(e), the SS-*g*-PAA shows three new characteristic absorption bands at 1618, 1445, and 1414 cm^{-1} verifying the formation of graft copolymer product. The SS-*g*-PAA hydrogel involves a salep sulfate backbone with side chains that carry carboxylic acid functional groups. Because the stretching band of C=O function in carboxylic acid groups overlaps with the carbonyl stretching of the salep sulfate portion of the copolymer, a broad signal is appeared around 1618 cm^{-1}.

In order to investigate the effect of sulfate substitution and grafting of AA onto the salep backbone, thermogravimetric analysis of samples were obtained. In Figure 3, the thermal gravimetric (TG) and Differential thermal gravimetric (DTG) curves for samples SS1, SS2, and SS3 compared to the parent salep are shown. All the TG curves indicate an initial weight loss up to 100°C, which is because of the adsorbed water on the polymers. The weight loss within the temperature of 300°C–450°C is attributed to the thermal decomposition of salep and salep sulfate. As can be observed, whenever the sulfate content increases the thermal stability of the sulfated polymer increases. The weight loss of parent salep is about 59% while the sulfate derivatives present losses lying between 8% and 16% depending on their substitution degree. The temperature of maximum weight loss which is attributed to the oxidative decomposition of the polymers follows the series SS1 < SS2 < S < SS3. The main reason for this behavior may be caused by the ordered structure destroyed during the sulfonating process. According to this TGA curves, values related to the parent salep around 250°C–400°C are lower compared to the salep-based hydrogel. Cross-linking structures may act as heat barriers, which delay the diffusion of both the volatile thermo oxidation products to the gas and oxygen from the gas phase to the polymer, and as a consequence, enhance the overall thermal stability of the hydrogel. At higher than 400°C, the salep was found to be the most thermally stable sample studied and this could be attributed to the nature of salep composition.[45,46]

Effect of Sulfate Content on Equilibrium Water Absorbency and Swelling Rate

The swelling degree of the hydrogel was measured in distilled water at consecutive time intervals. The swelling behavior of the hydrogels with various sulfate contents is represented in Figure 4. As shown in Figure 4, SS-*g*-PAA hydrogels need about 60 min to reach equilibrium water absorbency but S-*g*-PAA has higher swelling rate and need about 15 min to reach equilibrium water absorbency. This result indicates that sulfonation of salep decreases the swelling rate of corresponding hydrogels. It also can be seen from Figure 4 that the high equilibrium water absorbency is obtained when the sulfate content of salep sulfate is high. The variation of equilibrium water absorbency of the hydrogel with the sulfate content can be explained as follows. As the sulfate content increases, the hydrophilicity of salep sulfate increases which results in the higher equilibrium water absorbency of SS-*g*-PAA. In addition, with increasing the sulfate content, the osmotic pressure difference between the polymeric network and external medium increases which also contributes to the improvement of equilibrium water absorbency.

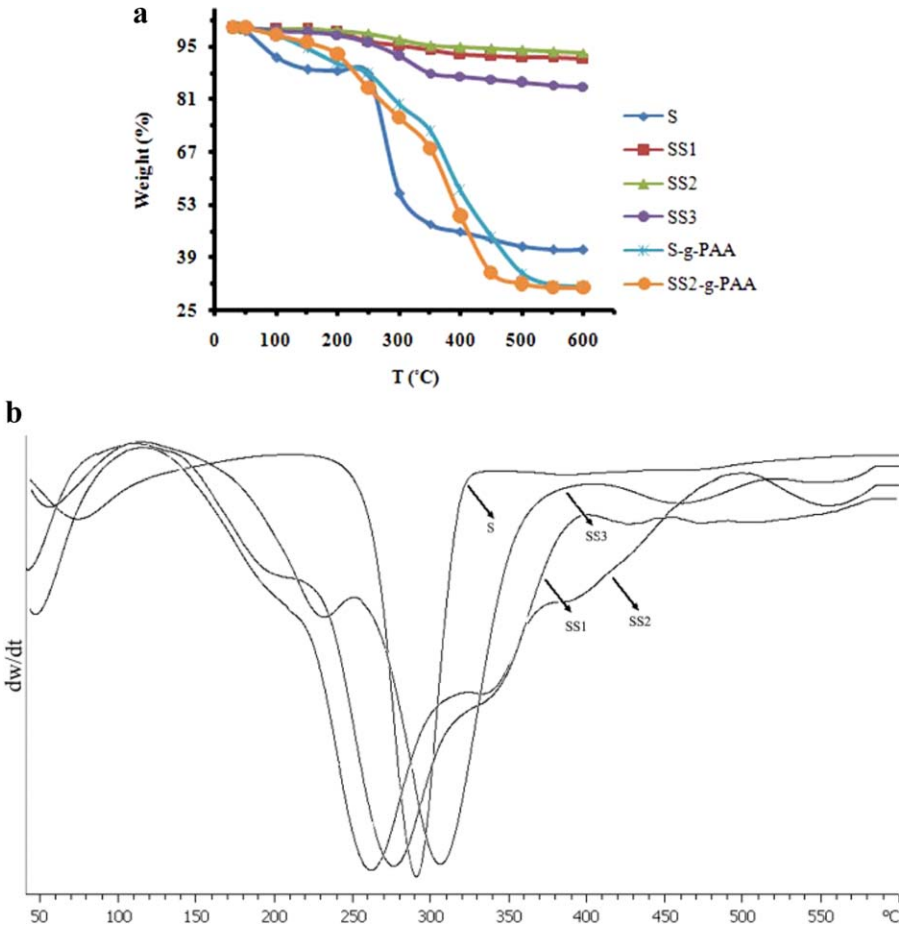

Figure 3. Thermogravimetric curves of parent salep, sulfated salep (SS1, SS2, and SS3), and hydrogels (S-*g*-PAA and SS2-*g*-PAA). [Color figure can be viewed in the online issue, which is available at wileyonlinelibrary.com.]

Effect of pH Solution on the Water Absorbency

In order to investigate the sensitivity of the synthesized hydrogels to pH, the equilibrium water absorbency of the hydrogels was studied at various pHs ranging from 3.0 to 12.0 [Figure 5(a)]. As can be seen from Figure 5(a), equilibrium water absorbency of the hydrogels depends on their sulfate substitution content and increases with increasing pH. In addition, salep-based hydrogel is fully expanded at pH 9 while equilibrium water absorbency of the SS-*g*-PAA hydrogels increases at pHs above 9. The main reason for this swelling behavior can be attributed to the deporotonation of sulfate substitutions at pHs above 9. When pH is increased, some sulfate and carboxylate groups are ionized and the electrostatic repulsion between them tends to expand the network. Whenever the sulfate substitution content increases, the equilibrium water absorbency at higher pH increases. As a result, SS2-*g*-PAA hydrogel shows the most equilibrium water absorbency at pH 12. Under acidic pHs, protonation of negatively charged groups attached to the polymer chains results to decrease in the main anion–anion repulsive forces and consequently swelling values are decreased.

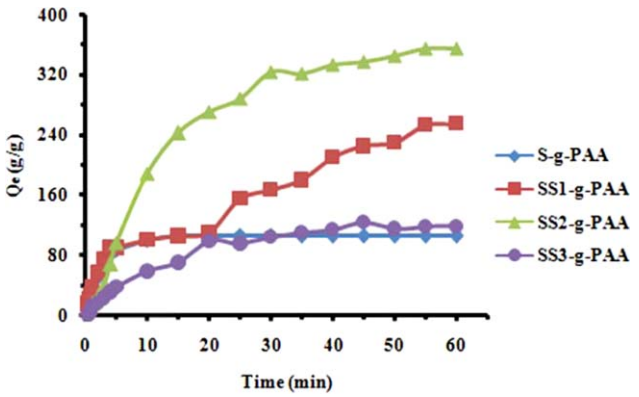

Figure 4. Effect of sulfate content on swelling kinetics of the hydrogels. [Color figure can be viewed in the online issue, which is available at wileyonlinelibrary.com.]

Effect of Salt Solution on Water Absorbency

The swelling behavior of the hydrogels in different concentrations of NaCl solution was investigated. Generally, the equilibrium water absorbency of ionic hydrogels in salt solutions is significantly decreased compared to distilled water. This phenomenon is related to a screening effect of the additional cations causing a nonefficient anion–anion electrostatic repulsion and commonly observed in the swelling of all ionic hydrogels.[47]

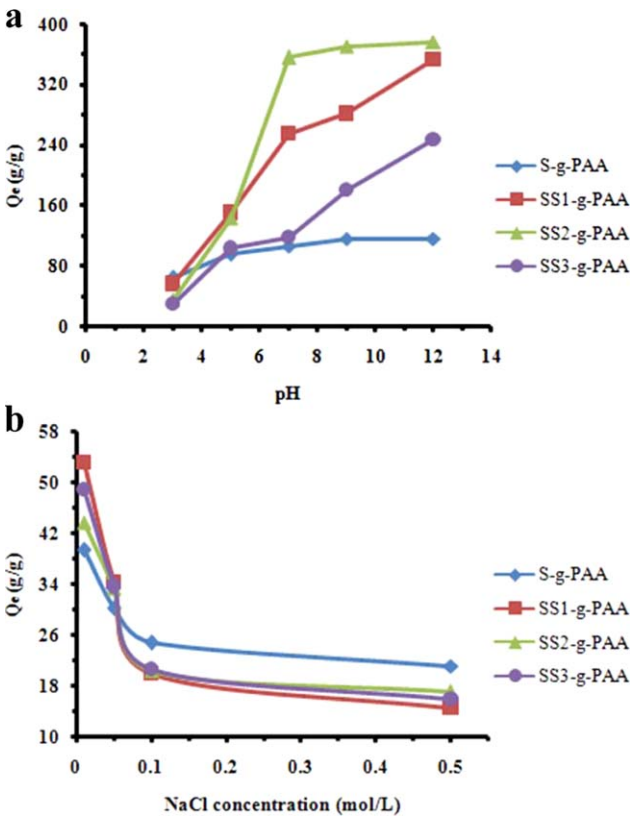

Figure 5. Swelling dependency of the hydrogels on pH (a) and concentration of NaCl (b) aqueous solution. [Color figure can be viewed in the online issue, which is available at wileyonlinelibrary.com.]

As can be seen from Figure 5(b), equilibrium water absorbency of the SS-*g*-PAA hydrogels is higher than that of S-*g*-PAA hydrogel when the salt concentration is less than 0.10 M. The main reason for this behavior may be attributed to that the sulfonation of salep increases osmotic pressure difference between the polymeric network and external saline solutions, and then the SS1-*g*-PAA hydrogel shows the highest equilibrium water absorbency in saline solutions (<0.10 M). With increasing saline concentration, swelling values for all above-mentioned hydrogels especially SS-*g*-PAA are expectedly decreased. This swelling loss is attributed to the charge screening effect increase of the cations that led to the reduction of osmotic pressure, the driving force for swelling, between the gel and the aqueous phase. It also can be seen from Figure 5(b), the decrease in equilibrium water absorbency of the SS-*g*-PAA hydrogels is higher than that of S-*g*-PAA hydrogel. The reason for this behavior can be attributed to that salt sensitivity of SS-*g*-PAA hydrogels is higher than S-*g*-PAA hydrogel.

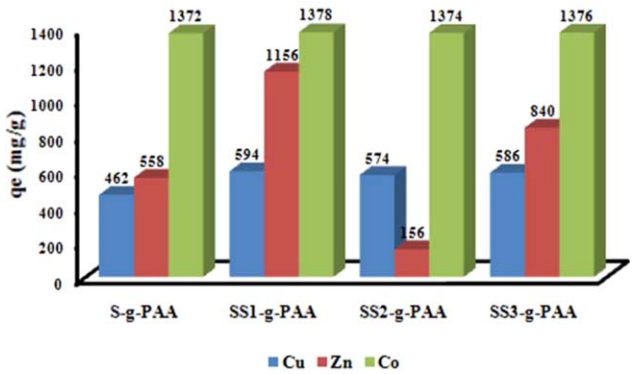

Figure 6. Effect of sulfate content on the metal ion adsorption capacities. [Color figure can be viewed in the online issue, which is available at wileyonlinelibrary.com.]

Studies on Sorption of Metal Ions

Figure 6 shows the influence of the sulfate content on adsorption of hydrogels for heavy metal ions at pH = 7. It is observed that the adsorption capacities of SS-*g*-PAA hydrogels are more than S-*g*-PAA hydrogel and SS1-*g*-PAA hydrogel has maximum heavy metal ion adsorption, which leads to the conclusion that the sulfate group participate in the heavy metal ions adsorption process. The adsorption capacities of salep sulfate-based hydrogels follow this order: SS1-*g*-PAA > SS3-*g*-PAA > SS2-*g*-PAA. A possible mechanism for metal ion binding to hydrogel is an ion-exchange mechanism, which involves an electrostatic interaction between metallic cations and negatively charged ligands. Thus, SS1-*g*-PAA hydrogel has suitable sulfate content for maximum electrostatic interaction with heavy metal ions. The decreasing adsorption capacity with sulfate content increasing evidently may be attributed to steric effect beyond a certain point and a dense complex formation on the surface of the hydrogel which prevent the diffusion of metal ions into the hydrogel. This phenomenon further suggests that the adsorption capacity of salep sulfate-based hydrogels not only depends on sulfate group but also on the other group with different affinity, such as –COOH and –OH group which have interaction or synergistic action for heavy metal ions adsorption.[48,49] The adsorption capacities of the SS1-*g*-PAA hydrogel are 1378 mg/g for Co(II), 594 mg/g for Cu(II), and 1156 mg/g for Zn(II). A brief comparison between metal ion adsorption capacities of salep sulfate-based hydrogel and some recently reported synthetic and bio-adsorbents is given

Table II. Adsorption Capacities (mg/g) of Metal Ions by Various Adsorbents

Adsorbents	Co^{2+}	Cu^{2+}	Zn^{2+}	Reference
Chitosan, itaconic, and methacrylic acid hydrogel		122.6		[50]
HPAM–chitosan gel beads		45		[51]
Chitosan/clinoptilolite	467.9			[52]
Carbon nanotube sheets	60	40	42	[53]
Modified plant wastes		90.9	83.3	[2]
Modified cellulose	20	60	27	[1]
Xylan-type hemicelluloses/AA hydrogel			274	[54]
SS1-*g*-PAA hydrogel	1378	594	1156	This work

in Table II. Cross-linked polymers, such as copolymers and hydrogels, usually show higher adsorption capacity because they possess a large amount of ligands and macro- or mesoporous structures. It is obvious from the data that the modified salep-based hydrogel prepared in the present work exhibits adsorption capacities much higher than that of either biopolymer-based or fully synthetic adsorbent. Overall, regarding the advantageous of salep as the starting material, cheapness of the reactants and reagents, facility of the processes, very high heavy metal ion adsorption capacity, and high adsorption rate, the salep-based hydrogel can be considered as an excellent candidate for water treatment purposes.

CONCLUSIONS

The present work shows that it was possible to prepare salep sulfate with different sulfate content using $HClSO_3$–DMF complex. The effect of reaction time and sulfating reagent on sulfate content of salep sulfate were investigated. ^{1}H NMR, FTIR spectra, and TGA curves showed the characterization of modified salep. The novel salep sulfate-based hydrogel was prepared by graft copolymerization of AA onto salep sulfate. The water absorbency of the prepared salep sulfate-based hydrogels was investigated in various media and compared with that of existing salep-based hydrogel. The enhanced water absorbency of salep sulfate-based hydrogel appears to be because of the increase in charge density and ionization tendency brought about by the introduction of sulfate anions, in addition to the carboxylate anion in salep-based hydrogel. The heavy metal ion adsorption capacity of the prepared hydrogel can be controlled by adjusting the amount of sulfate groups on adsorbents, which is proportional to the adsorption capacity.

REFERENCES

1. O'Connell, D. W.; Birkinshaw, C.; O'Dwyer, T. F. *Bioresour. Technol.* **2008**, *99*, 6709.
2. Wan Ngah, W. S.; Hanafiah, M. A. K. M. *Bioresour. Technol.* **2008**, *99*, 3935.
3. Djedidi, Z.; Bouda, M.; Souissi, M. A.; Cheikh, R. B.; Mercier, G.; Tyagi, R. D.; Blais, J. F. *J. Hazard. Mater.* **2009**, *172*, 1372.
4. Domanska, U.; Rekawek, A. *J. Solution Chem.* **2009**, *38*, 739.
5. Cojocaru, C.; Zakrzewska-Trznadel, G.; Jaworska, A. *J. Hazard. Mater.* **2009**, *169*, 599.
6. Rafati, L.; Mahvi, A. H.; Asgari, A. R.; Hosseini, S. S. *Int. J. Environ. Sci. Tech.* **2010**, *7*, 147.
7. Guo, Z. J.; Su, H. Y.; Wu, W.S. *Radiochim. Acta* **2009**, *97*, 133.
8. Weng, C. H.; Huang, C. P. *Colloid Surf. A* **2004**, *247*, 137.
9. Biscup, B.; Subotic, B. *Sep. Sci. Technol.* **2004**, *39*, 925.
10. Sublet, R.; Simonnot, M. O.; Boireau, A.; Sardin, M. *Water Res.* **2003**, *37*, 4904.
11. Arias, M.; Barral, M. T.; Mejuto, J. C. *Chemosphere* **2002**, *48*, 1081.
12. Feng, D.; van Deventer, J. S. J.; Aldrich, C. *Sep. Purif. Technol.* **2004**, *40*, 61.
13. Abdel-Halim, E. S.; Al-Deyab, S. S. *Carbohyd. Polym.* **2011**, *86*, 1306.
14. Demirbilek, C.; Dinc, C. O. *Carbohyd. Polym.* **2012**, *90*, 1159.
15. Li, W.; Zhao, H.; Teasdale, P. R.; John, R.; Zhang, S. *React. Funct. Polym.* **2002**, *52*, 31.
16. Paulino, A. T.; Guilherme, M. R.; Mattoso, L. H. C.; Tambourgi, E. B. *Macromol. Chem. Phys.* **2010**, *211*, 1196.
17. Dorkoosh, F. A.; Verhoef, J. C.; Borchard, G.; Rafiee-Tehrani, M.; Verheijden, J. H. M.; Junginger, H. E. *Inter. J. Pharm.* **2002**, *247*, 47.
18. Dorkoosh, F. A.; Verhoef, J. C.; Ambagts, M. H. C.; Rafiee-Tehrani, M.; Borchard, G.; Junginger, H. E. *Eur. J. Pharm. Sci.* **2002**, *15*, 433.
19. Lim, D. W.; Whang, H. S.; Yoon, K. J.; Ko, S. W. *J. Appl. Polym. Sci.* **2001**, *79*, 1423.
20. Peng, G.; Xu, S.; Peng, Y.; Wang, J.; Zheng, L. *Bioresource Technol.* **2008**, *99*, 444.
21. Zhang, J.; Li, A.; Wang, A. *Carbohyd. Polym.* **2006**, *65*, 150.
22. Kaya, S.; Tekin, A. R. *J. Food Eng.* **2001**, *47*, 59.
23. Vuksan, V.; Jenkins, D. J.; Spadafora, P.; Sievenpiper, J. L.; Owen, R.; Vidgen, E. *Diabetes Care* **1999**, *22*, 913.
24. Reffo, G. C.; Ghirardi, P. E.; Forattani, C. *Curr. Ther. Res.* **1990**, *47*, 753.
25. Marzio, L.; Bianco, R. D.; Donne, M.; Pieramico, O.; Cuccurullo, F. *Am. J. Gastroenterol.* **1989**, *84*, 888.
26. Hozumi, T.; Yoshida, M.; Ishida, Y.; Mimoto, H.; Sawa, J.; Doi, K.; Kazumi, T. *Endocrine J.* **1995**, *42*, 187.
27. Pourjavadi, A.; Rezanejade Bardajee, G.; Soleyman, R. *J. Appl. Polym. Sci.* **2009**, *112*, 2625.
28. Pourjavadi, A.; Doulabi, M.; Soleyman, R.; Sharif, S.; Eghtesadi, S. A. *React. Funct. Polym.* **2012**, *72*, 667.
29. Pourjavadi, A.; Soleyman, R.; Rezanejade Bardajee, G. *Starch/Starke* **2008**, *60*, 467.
30. Rezanejade Bardajee, G.; Pourjavadi, A.; Soleyman, R.; Sheikh, N. *Nucl. Instrum. Methods Phys. Res. Sect. B* **2008**, *266*, 3932.
31. Rezanejade Bardajee, G.; Pourjavadi, A.; Ghavami, S.; Soleyman, R.; Jafarpour, F. *J. Photochem. Photobiol. B* **2011**, *102*, 232.
32. Saeidian, H.; Matloubi Moghaddam, F.; Pourjavadi, A.; Barzegar, S.; Soleyman, R.; Sohrabi, A. *J. Braz. Chem. Soc.* **2009**, *20*, 466.
33. Shaabani, A.; Rahmati, A.; Badri, Z. *Catal. Commun.* **2008**, *9*, 13.
34. Alban, S.; Franz, G. *Thromb. Res.* **2000**, *99*, 377.
35. Rajalaxmi, D.; Leslie, N. G.; Ragauskas, A. J. *Carbohyd. Res.* **2010**, *345*, 284.
36. Xing, R.; Liu, S.; Yu, H.; Zhang, Q.; Li, Z.; Li, P. *Carbohyd. Res.* **2004**, *339*, 2515.
37. Vongchan, P.; Sajomsang, W.; Subyen, D.; Kongtawelert, P. *Carbohyd. Res.* **2002**, *337*, 1239.

38. Wang, Z. M.; Li, L.; Zheng, B. S.; Normakhamatov, N.; Guo, S. Y. *Int. J. Biol. Macromol.* **2007**, *41*, 376.
39. Schweiger, R. G. *Carbohyd. Res.* **1972**, *21*, 219.
40. Gamzazade, A.; Skyyar, A.; Nasibov, S.; Suskov, A.; Knirel Yu, A. *Carbohyd. Polym.* **1997**, *34*, 113
41. Kannamba, B.; Laxma Reddy, K.; AppaRao, B. V. *J. Hazard. Mater.* **2010**, *175*, 939.
42. Pourjavadi, A.; Harzandi, A. M.; Hosseinzadeh H. *Eur. Polym. J.* **2004**, *40*, 1363.
43. Hsu, S. C.; Don, T. M.; Chiu, W. Y. *Polym. Degrad. Stab.* **2002**, *75*, 73.
44. Bajpai, S. K.; Johnson, S. *React. Funct. Polym.* **2005**, *62*, 271.
45. Farhoosh, R.; Riazi, A. *Food Hydrocolloid.* **2006**, *20*, 660.
46. Tekinsen, K. K.; Guner, A. *Food Chem.* **2010**, *121*, 468.
47. Buchholz, F. L.; Graham, A. T. Modern Superabsorbent Polymer Technology; Wiley-VCH: New York, **1998**; p 1.
48. Kadirvelu, K.; Faur-Brasquet, C.; Le Cloirec, P. *Langmuir* **2000**, *16*, 8404.
49. Sun, S.; Wang, A. *React. Funct. Polym.* **2006**, *66*, 819.
50. Milosavljevic, N. B.; Ristic, M. D.; Peric-Grujic, A. A.; Filipovic, J. M.; Strbac, S. B.; Rakocevic, Z. L.; Kalagasidis Krusic, M. T. *Colloid Surf. A* **2011**, *388*, 59.
51. Cao, J.; Tan, Y.; Che, Y.; Xin, H. *Bioresour. Technol.* **2010**, *101*, 2558.
52. Dinu, M. V.; Dragan, E. S. *Chem. Eng. J.* **2010**, *160*, 157.
53. Ahmadzadeh Tofighy, M.; Mohammadi, T. *J. Hazard. Mater.* **2011**, *185*, 140.
54. Peng, X. W.; Zhong, L. X.; Ren, J. L.; Sun, R. C. *J. Agr. Food Chem.* **2012**, *60*, 3909.